Implementation of a novel continuous solid/liquid mixing accessory for 3D printing of dysphagia-oriented thickened fluids

I. Diañez[a], C. Gallegos[b], E. Brito-de la Fuente[b], I. Martínez[a], C. Valencia[a], M.C. Sánchez[a], J.M. Franco[a,✉]

[a] Pro²TecS – Chemical Process and Product Technology Center. Dpto. Ingeniería Química. ETSI. Campus de "El Carmen". Universidad de Huelva. 21071, Huelva. Spain.

[b] Product & Process Engineering Centre, Fresenius Kabi Deutschland GmbH, 61352 Bad Homburg, Germany

ABSTRACT

This paper describes the implementation and evaluation of an accessory designed and manufactured to be adapted to a 3D printer to allow the in situ and continuous mixing of powder and liquid feeds. In particular, the capacity of this accessory to correctly mix a dysphagia-oriented commercial powder thickener with several conventional fluids (i.e. water, juice, and milk) was studied. Target thickener concentrations were defined in order to achieve mixtures with viscosities corresponding to the textures established by the National Dysphagia Diet Task Force (NDD)—nectar-like, honey-like, and spoon-thick—for thickened fluids. Both the accuracy of the solid content and the rheological response of the obtained mixtures were evaluated. Although fluctuations were observed in the concentrations of the mixtures obtained by continuous mixing with respect to the target values, the viscosities obtained were within the limits established for each of the desired textures. The thickened fluids processed using the 3D printing mixing accessory showed viscosities very similar to their hand-mixed counterparts and a higher degree of structuration, especially when printed at low mass flow rates, as well as a lower amount of entrapped air. This method of preparation allows the production of thickened fluids with more appealing shapes and colours for the long-term dysphagia management, improving the quality of life of patients with dysphagia, and promoting treatment compliance.

Keywords: 3D printing; dysphagia; gels; mixing; thickened fluids; rheology.

1. Introduction

Swallowing difficulty (dysphagia) is a problem that, according to the most conservative estimates, affects approximately 8% of the world's population (Cichero et al., 2013). Dysphagia can be a consequence of a multitude of neurological, muscular, and structural pathologies or can even be drug-induced (Shaker, 2006). It can lead to very serious complications, including malnutrition and

dehydration as well as severe respiratory problems, such as aspiration pneumonia, resulting from the aspiration of food or fluids into the airways (Carrión et al., 2019; Pere Clavé & Shaker, 2015). As a result, dysphagia is associated with increased morbidity, worse prognoses, longer hospital stays, more frequent readmissions, and, in turn, higher mortality rates (Attrill et al., 2018; Cabré et al., 2013).

One of the most widely used interventions in the management of dysphagia is the thickening of low-viscosity liquids, as these normally present the greatest risk of aspiration (Andersen et al., 2013; Newman et al., 2016). Fresubin® Clear Thickener (FCT) is a gum-based α-amylase-resistant powder thickener that is widely used for modifying the rheological behaviour of fluids in dysphagia management (Ortega et al., 2020; Turcanu et al., 2018). As the thickener increases the viscosity of the fluids, the flow rate of the bolus during swallowing is significantly reduced, increasing the chances of the airways being secured in time to prevent aspiration (Inamoto et al., 2013; Qazi et al., 2019). The viscosity-dependent therapeutic effect of this thickener has proven to be especially noticeable in patients with impaired swallowing physiology, such as elderly people, Parkinson's disease patients and post-stroke patients. Increasing viscosity through the use of this thickener allows these patients to swallow safely in up to 96% of cases, compared to just over 40% who are able to do so when swallowing low-viscosity liquids (Ortega et al., 2020). As the viscosity required for safe swallowing varies from patient to patient (Choi et al., 2011; P. Clavé et al., 2006), several levels of thickening are established. The most common and accepted classification is that given by the National Dysphagia Diet Task Force (NDD); according to this classification, at a shear rate of 50 s^{-1} and a temperature of 25 °C the viscosity values are as follows (American Dietetic Association, 2002):

- Thin liquid: 1–50 mPa·s
- Nectar-like: 51–350 mPa·s
- Honey-like: 351–1750 mPa·s
- Spoon-thick: <1750 mPa·s

However, although this classification has been widely used for years, it is not universally accepted at the level of the medical community, as it is excessively simplistic and does not consider the non-Newtonian character of these thickened fluids or the different effective shear rates along the upper digestive tract (Brito-de la Fuente et al., 2019; Nutritional Aspects of Dysphagia Management, 2017; Salinas-Vázquez et al., 2014). In addition, the influence of saliva in the rheological properties of these thickened products should also be taken into account to improve the management of dysphagia (Herranz et al., 2021). All this has led to the emergence of different initiatives to implement viscosity level classifications that do consider these aspects, such as the one promoted by the European Society for Swallowing Disorders (ESSD) in alliance with other relevant European societies. This

initiative recommends that, in addition to texture classification at 50 s^{-1}, manufacturers of thickening agents also include the viscosity value, at 300 s^{-1}, in mPa·s into the labels, as well as the effect on it of salivary α-amylase (Baijens et al., 2021).

FCT-thickened fluids show a well-known and characterised shear-thinning behaviour, with a reduction in viscosity of around two decades when shear rate is increased from 1 to 300 s^{-1}. Additionally, in contrast to other thickeners, FCT-thickened fluids are not affected by α-amylase, with the same shear-induced viscosity reduction observed in orally incubated samples as in the absence of saliva. This is an essential feature for dysphagia-oriented products, as a significant reduction in viscosity on contact with saliva can seriously compromise patient safety (Ortega et al., 2020; Turcanu et al., 2018).

The dose of FCT required to obtain these consistencies (nectar-like and higher) starting from Newtonian fluids as well as the way to prepare thickened liquids by manual mixing are indicated on the FCT packaging. However, although these instructions indicate how to reduce the inlet of air and consequent formation of bubbles in the mixture as much as possible, this is almost impossible in manual mixing and even more difficult with other mechanical means (such as blenders) (Sopade, Halley, Cichero, Ward, Hui, et al., 2008). Furthermore, it can be difficult for this process to be repeated from one preparation to another, especially if mixing is performed by different people. These complications, in the worst case, can lead to a significant decrease in the viscosity of the mixture, thus the failure to meet the specific requirements for each texture.

To minimise these drawbacks while providing new and interesting features, in this study, a new mixing device was designed and manufactured to be adapted to a 3D printer and controlled by its firmware, allowing the continuous and automatic in situ mixing of (at least) one powder and one liquid feed. This device can simply be used as an automatic mixer to obtain mixtures with proportions controlled via software. In this way, it exhibits advantages over manual preparation, because the introduction of air into the system during manual mixing is unavoidable (especially in mixtures with high viscosity). This new preparation method allows mixing without letting air enter the system; the few small air bubbles that can be observed in mixtures are due solely to the air trapped between the solid particles, which can be minimised by controlling the granulometry.

In addition, through the use of additional feeds, more complex mixtures containing nutrients, drugs, or even colouring and/or flavouring agents can be prepared. When used to obtain concentrated systems (>10 wt.%) with viscosities that allow self-sustainment to form three-dimensional configurations, shape can be another key element in making thickened fluids more palatable and appealing for dysphagia patients. With the device coupled to a 3D printer, which allows it to be moved in three dimensions, gel models can be designed and printed with appealing shapes similar to

conventional foods, which could make clinical nutrition more attractive to patients and less repetitive in long-term treatments (Diañez et al., 2019). Making thickened fluids more attractive is of utmost importance, as the lack of acceptance of these products by patients is a well-known issue. Patients' dislike of thickened fluids has, on the one hand, a very significant negative effect on their quality of life and, on the other hand, negative effects due to the potential non-compliance with treatment or reduced fluid and food intake (Colodny, 2005; Lim et al., 2016; Low et al., 2001).

The objective of this study was to develop and validate a novel device designed for the continuous mixing of solids and liquids, hereinafter referred to as the MIX3D accessory, controlled by the firmware of a RepRap 3D printer to which it is attached in order to be applied for dysphagia management. This device can mix a liquid (water, juice, and milk) with FCT to obtain mixtures at different concentrations covering the range from nectar-like to spoon-thick consistencies. The actual content of solids and the final rheological behaviour of the mixtures obtained with the proposed device were evaluated and compared with those found in hand-prepared mixtures by following the instructions given on the label of the product.

2. Experimental

2.1. Materials

FCT was provided by Fresenius Kabi Deutschland GmbH (batch 29NB0433). This commercial thickener, widely used in dysphagia management, is composed of xanthan gum, modified starch, maltodextrin, modified cellulose and flavouring (Ortega et al., 2020). The nutritional information is included in Table 1.

Table 1. Nutritional information for Fresubin® Clear Thickener (*Fresubin Clear Thickener – Caring for Life*, n.d.)

Ingredients	Average content per 100g
Energy [kJ/kcal]	1108/264
Fat [g]	0
Carbohydrate [g]	41.5
of which sugar [g]	1.3
of which lactose [g]	0
Fibre [g]	48
Protein [g]	0.5
Sodium [mg/mmol]	1570/68.3
Potassium[mg/mmol]	500/12.8
Phosphorus[mg/mmol]	200/6.5

and used as received to be fed into the hopper of the MIX3D accessory for subsequent mixing with distilled water. Orange juice with no added sugar (Juver SA, Spain) and skimmed milk (Covap, Spain), purchased in a local store, were also used as alternative solvents.

2.2. 3D printer

The BQ Hephestos 3D printer DIY kit designed by BQ (Spain) and the electronics (Arduino Mega 2560 and RAMPS 1.4 shield) were purchased from Ícarus Informática (Spain). All parts of the MIX3D accessory (excluding stepper motor and screws) were designed in our laboratory and printed with an unmodified BQ Hephestos.

Marlin was chosen as firmware for the 3D printer. The different models printed during this study were designed using the AutoCAD 2018 software and Tinkercad online app. The 3D models were sliced using the Ultimaker Cura software, and the 3D printer was controlled during operation using the Repetier-Host software.

To mix solids and liquids during printing, the equipment must handle both types of feeds separately. The liquid feed is dosed using a syringe pump driven by a motor directly connected to the printer electronics to be controlled as a conventional extruder (Figure 1a). This syringe pump was also designed and assembled from 3D printed parts and non-printable components supplied by 3DEspana (Spain). The solid, in powder form, is fed through a hopper and dosed by a feeder screw, which will also drive and mix the material during its flow through the MIX3D accessory (Figure 1b). More detailed drawings and the dimensions of the mixing chamber, the screw and the hopper can be found in the Supporting Information (Figure S1).

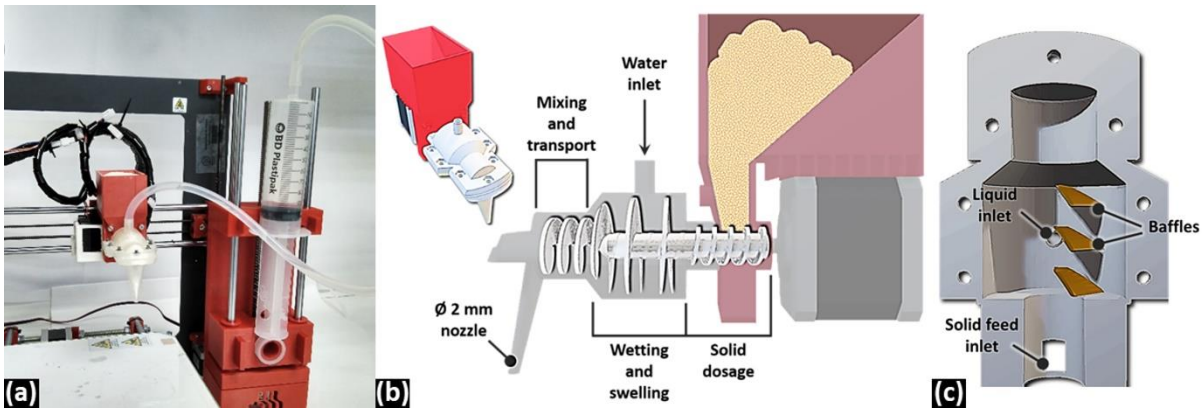

Figure 1. MIX3D accessory layout. (a) photograph of device and syringe pump setup, (b) schematic representation of the mixing device, (c) inside view of the upper half of the mixing device casing

The mixing screw is directly attached and driven by a NEMA 17 motor, which, like the one in the syringe pump, is configured as a conventional extruder to be controlled via software. Marlin firmware has the option of using a mixing extruder, by uncommenting the option available in the 'Configuration.h' file and specifying the number of motors to be used. The extruders can then be operated simultaneously through a virtual extruder in Repetier-Host for which the flow ratio of both feeds can be controlled by means of a simple script. However, when a conventional 3D printer has multiple extruders, they are usually of the same type and geometry, so the flow ratio can be

assigned directly. That is, by setting a weight of 50 (over 100) for each extruder, the material flow would be the same. This is not the case in the proposed system, where the syringe pump and hopper are feeding systems with completely different geometries; for equal motor movement, they provide different material flows. Therefore, the first step to set a specific concentration is to calibrate each of the feeds passing through the system individually. Once each feed has been calibrated separately, it is possible to correct the weights and obtain the desired solid content.

The casing of the device is divided into two halves (upper and lower) to allow the insertion and removal of the screw as well as the cleaning of all components. The feeding inlets are located in the upper half to reduce the probability of clogging, while the mixing outlet is located at the end of the lower half. In addition, the upper part contains an array of baffles (Figure 1c) matching the truncated segments of the screw for the removal of the wet solid from the surface of the screw. The device has no heating or cooling system, so prints were performed at room temperature.

All parts of the mixing device must be perfectly clean and dry before assembly. The two casing halves were secured with screws after inserting the feeder screw. This whole set is coupled to the hopper so that the motor shaft fits with the cavity in the feeder screw. Then, the hopper is loaded with the FCT powder, and the syringe pump, previously loaded with the liquid to be thickened, is connected to the upper inlet of the casing. When the device is loaded and ready for use, the desired flow ratio is configured via software.

It is worth mentioning that the weight of the device as a whole, even when filled with material, is very similar to that of the original Hephestos extruder (around 470 and 485 g, respectively). This is an important detail, as loading the 3D printer carriage with heavy components can be a source of problems during printing, as well as shortening the lifespan of mechanical components.

2.3. Calibration of the device and printing parameters

The firmware of the printer measures the advance of the motors (their rotation) in units of length. Thus, by setting the printer to print different distances and weighing the amount of material printed in each case, a flow rate value in g/mm can be obtained. This flow rate value, in turn, can be converted into the mass flow rate directly by means of the printing speed used (Eq. 1):

$$\dot{m} = fr \cdot v \,, \tag{1}$$

where $\dot{m}$ is the mass flow rate [g/min], fr is the flow rate [g/mm], and v is the printing speed [mm/min].

Since the geometries of the two feed systems are different, as are the flow rate values for the solvent (fr_s) and the solid (fr_{FCT}), therefore each of the flows has to be calibrated independently by

189 weighing the amount of material supplied by the syringe pump and the screw for given motor
190 advance lengths, resulting in:

$$fr_{FCT} = 1.13 \cdot \frac{10^{-3} g}{mm}, \qquad fr_s = 0.33 \frac{g}{mm}.$$

191 Once the characteristic flow rate of each feed system is known, a weight from 0 to 100 is applied to
192 each motor to control the mixing ratio. A weight of 1 was assigned to the syringe pump motor (w_s),
193 as it was the one with the highest feeding capacity. Then, the weight for the motor driving the screw
194 (w_{FCT}) was calculated to obtain the correct ratio in each case. However, the sum of the weights of
195 the different motors must be equal to 100, so that a third 'ghost' motor is defined in order to absorb
196 the excess weights. Different mass flows can be achieved by multiplying the weights of the FCT and
197 solvent. For instance, considering the nectar-like concentration (1.6 wt.%),

198 $$\dot{m} = 2\ g/min \begin{cases} w_s = 1 \\ w_{FCT} = 4, \\ w_g = 95 \end{cases} \qquad \dot{m} = 4\ g/min \begin{cases} w_s = 2 \\ w_{FCT} = 8\ , \\ w_g = 90 \end{cases}$$

199 where w_s, w_{FCT}, and w_g are the weights of the solvent feeding motor, the FCT feeding motor, and
200 "ghost" motor, respectively. The script to apply these mixing ratios in Repetier-Host would then be
201 as shown below for the example of the nectar-like texture at 2 g/min:

```
202 M163 S0 P1
203 M163 S1 P4
204 M163 S2 P95
205 M164 S0
206 T0
```

207 This script saves these mixing ratios for extruder 0 and selects the corresponding extruder (T0).
208 There are several ways for this script to be applied during printing, but the most convenient is to add
209 it in Cura as part of the 'Start G-code' field in the machine settings.
210 Finally, the mixing mass flow rate can be calculated as follows:

$$\dot{m} = (w_{FCT} \cdot fr_{FCT} + w_s \cdot fr_s) \cdot v. \qquad (2)$$

211 The printing speed was set to 600 mm/min for nectar-like blends and was slightly changed to
212 compensate for the increased solid flow for the two higher concentrations. The resulting
213 configurations for each concentration and mass flow are summarised in Table 2.
214

Table 2. Summary of the samples studied in this work

Texture	FCT concentration setpoint [wt.%][a]	Printing speed [mm/min]	w_s/w_{FCT}	Mass flow rate [g/min]
Nectar-like	1.6	600	1/4	2
			2/8	4
			3/12	6
			5/20	10
Honey-like	5.0	583	1/13	2
			2/26	4
			3/39	6
			4/52	8
Spoon-thick[b]	9.5	555	1/26	2
			2/52	4

[a] Manufacturer's recommended concentrations, indicated on product packaging

[b] The same mass flow rates have not been studied for all textures because, with shorter residence times, the mixing was not adequate, and very heterogeneous systems were obtained

However, owing to the high viscosity and stickiness of the system, the complexity in the mixing and flow of the material causes fluctuations in the final concentration. One of the goals of this work was to optimise the operating parameters and routines of the device to improve the accuracy of the concentrations obtained and thus ensure that the resulting thickened fluids had the right viscosity for each texture. Thus, the actual solid content of each sample was gravimetrically quantified. To this end, each sample was weighed before being placed in a Selecta Digitronic convection oven (Selecta SA, Spain), dried overnight at 90 °C, and weighed again the day after.

Once the flow rates and concentrations have been optimised, the device can be used for different purposes. For thickened fluids with lower concentrations (nectar-like and honey-like textures), the device would basically act as an automatic dispenser or as a way to create decorations that do not require the material to be able to form self-sustaining structures. When the mixed products have sufficient consistency to self-support, as is the case of spoon-thick textures, the potential of 3D printing is really exploited, and attractive forms and/or shapes that simulate real food can be created, as shown in Figure 2 and Movie M1 of the Supporting Information.

Although only concentrations corresponding to NDD textures have been systematically studied, blends at 20 wt.% FCT (2 g/min mass flow) have been achieved with acceptable repeatability, giving viscosities of around 575 Pa·s at 0.5 s^{-1} and 9 Pa·s at 50 s^{-1}.

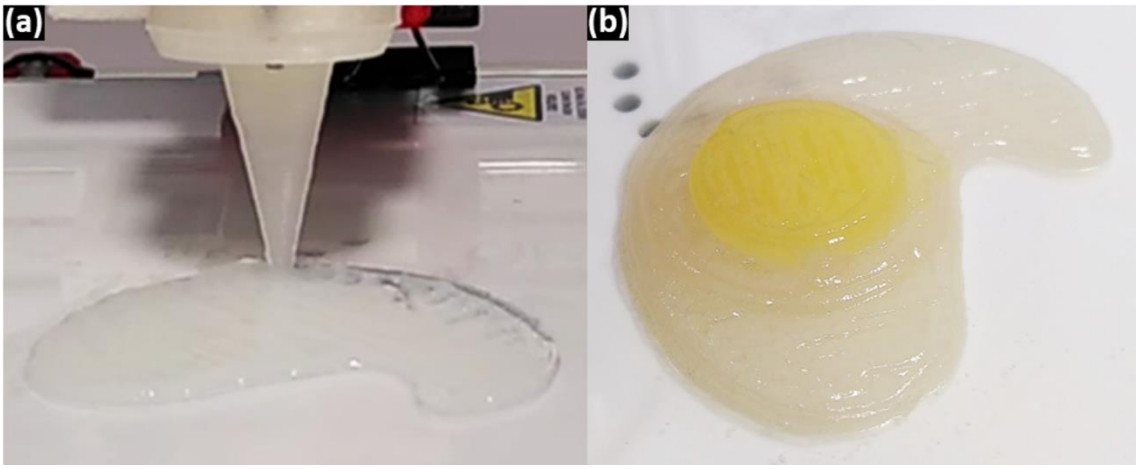

Figure 2.·3D printing of a simulated fried egg made with thickened milk and orange juice (a) during and (b) after 3D printing (FCT concentration: 9.5% wt.).

2.4. Rheological characterisation

Rheological characterisation of the MIX3D accessory-processed prints was carried out with a controlled stress rheometer (Physica MCR-301, Anton Paar, Austria). Viscous flow measurements were performed within a range of shear rates of 0.01–100 s^{-1} at 25 °C using a 50 mm serrated plate geometry and a gap of 1 mm.

The same plate-plate geometry was used to perform small-amplitude oscillatory shear (SAOS) tests inside the linear viscoelastic region in a frequency range of 100–0.03 rad/s.

2.5. Statistical Analysis

For the evaluation of concentration accuracy, the solids content of at least seven samples was checked for each texture and flow rate. Among them, a minimum of eight samples (at least two at each flow rate) per level of consistency were subjected to viscous flow measurements, and four samples (two per flow rate) were subjected to SAOS tests. The standard deviation was calculated for each mean value as a measure of variability.

3. Results and discussion

3.1. Solid content accuracy

The first step in the evaluation of the applicability of the MIX3D accessory is to check that the concentrations obtained are correct according to the setpoint established via software in each case. Although this may seem trivial because the feeds have been correctly calibrated separately and without fluctuations in their flow, it is not. When FCT and water come into contact, a very sticky, highly viscous wet dough is created, whose flow properties change as it moves through the

accessory and the degree of mixing increases. In addition, this process significantly depends on the concentration set. The handling of this wet dough is very complex and has led to numerous changes in the design of the device to avoid blockages, accumulations of solids, and total or partial clogging of the feed inlets, which were the main reasons why the concentrations obtained were very different from those expected. While the current design solves all these complications, there are still some fluctuations and variations in concentration among printed replicates. Figure 3 shows the actual concentrations of all the blends processed with the MIX3D accessory throughout this study, and their deviation from the target concentrations.

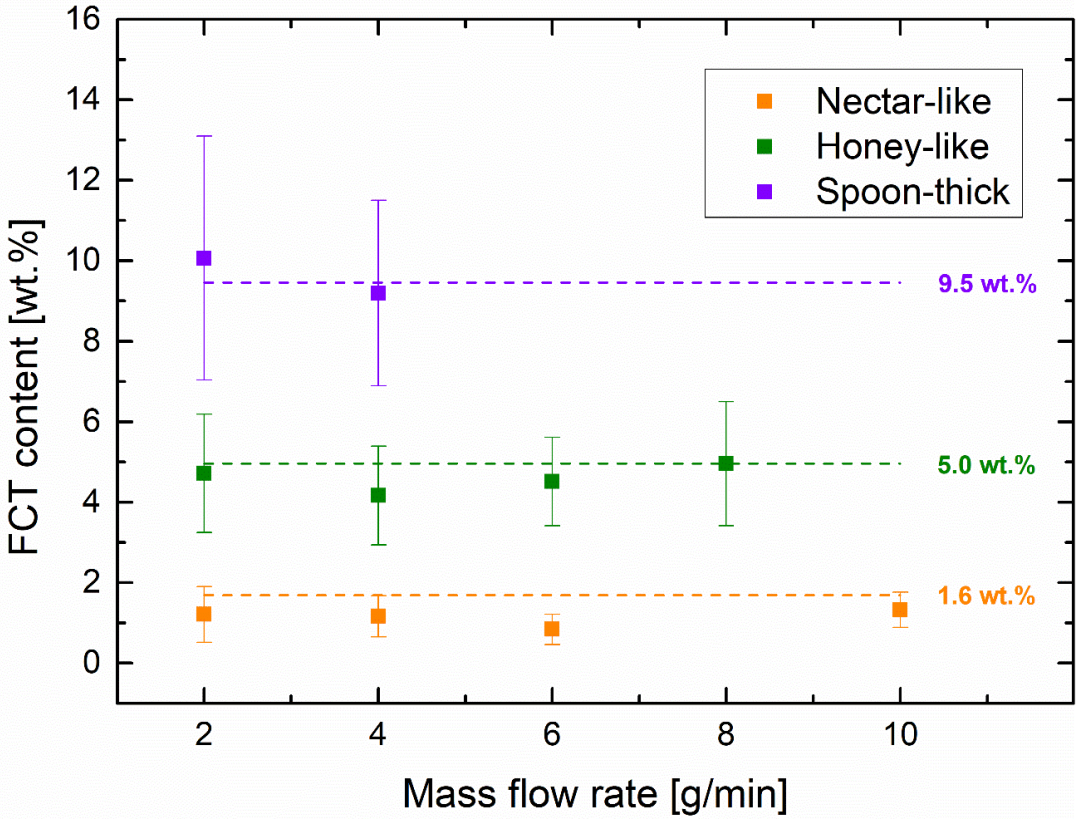

Figure 3. Actual FCT content of thickened water obtained with the MIX3D accessory at different mass flow rates

The figures illustrate the complexity of the flow of the solid/liquid blend and its dependence on concentration, as discussed previously. At all flow rates, the average solid content of the nectar-like blends was 1.1 ± 0.5 wt.%. The variability among the concentrations obtained was minimal in this case. However, this value is slightly lower than the target value. At all mass flows, the mean concentration values for honey-like and spoon-thick textures were 4.5 ± 1.3 and 9.6 ± 2.6 wt.%, respectively. For these consistencies, the variability was greater. Nevertheless, the averages are proportionally much closer to the set value, especially in the case of the spoon-thick blends. The sources of error in the concentration, as observed during the experimentation with the device, are the backward movement of liquid into the dry solid feed zone (Figure 1) and the slight accumulation of solid stuck to the different elements of the accessory. In the first case, the moistened powder in

the feed zone causes a reduction in the flow of the solid, which results in a concentration drop. In fact, this is most likely the cause of the average solids content below the setpoint for nectar- and honey-like textures, as the lower linear velocity induced by the screw and the presence of a greater amount of water within the device induces the liquid to flow back more easily. In the second case, the solid accumulated in the small dead zones of the device causes the concentration to be slightly lower at the beginning of the operation and higher afterwards. However, the variation caused by this effect is minor (the device is designed to minimise dead zones and baffles avoid the adhesion of solid to the surface of the screw) and is only noticeable for the more concentrated blends (spoon-thick samples) since, in those with a higher water content, the powder dissolves better and does not accumulate.

Figure 3 also shows that, for nectar- and honey-like textures, the concentrations are more accurate at both low (2 g/min) and high (8 or 10 g/min, depending on the case) flow rates, with intermediate flows being more distant from the setpoint. At low rates, the residence time is higher and the powder is better dissolved in most of its path. When the solid is properly dissolved, the gel formed is not sticky, as in the case of the initial mixture; instead, it is slippery and flows easily. On the other hand, at high flow rates, the rapid linear advance of the screw rotating at high speed prevents the liquid from flowing back into the dry solid feeding zone, which has already been described as one of the most common complications. Thus, the intermediate flow values, in which none of these favourable situations occur, are those that present the greatest difficulty; thus, they are the values that are generally farthest from the setpoint.

3.2. Flow measurements

One of the main goals of the design of products for patients with dysphagia is to meet the prescribed requirements in terms of viscosity/consistency for a safe swallowing process. The addition of beverages and foods with inadequate viscosity increases the risk of aspiration and poses a real threat to their health, especially when the viscosity is lower than specified, as most patients with dysphagia have more problems swallowing thin liquids (Bolivar-Prados et al., 2019; Nutritional Aspects of Dysphagia Management, 2017; Leonard et al., 2014; Newman et al., 2016; Ortega et al., 2020; Quinchia et al., 2011).

Figure a shows the viscosity values of FCT/water blends processed with the MIX3D accessory measured at 50 s^{-1} and 25 °C (η_{50}) according to NDD criteria. The largest points correspond to the average values and their standard deviations from the values obtained for each target concentration setpoint (1.6, 5.0, and 9.5 wt.%). On the other hand, black unfilled points refer to η_{50} values measured for hand-prepared blends, i.e. the conventional preparation method.

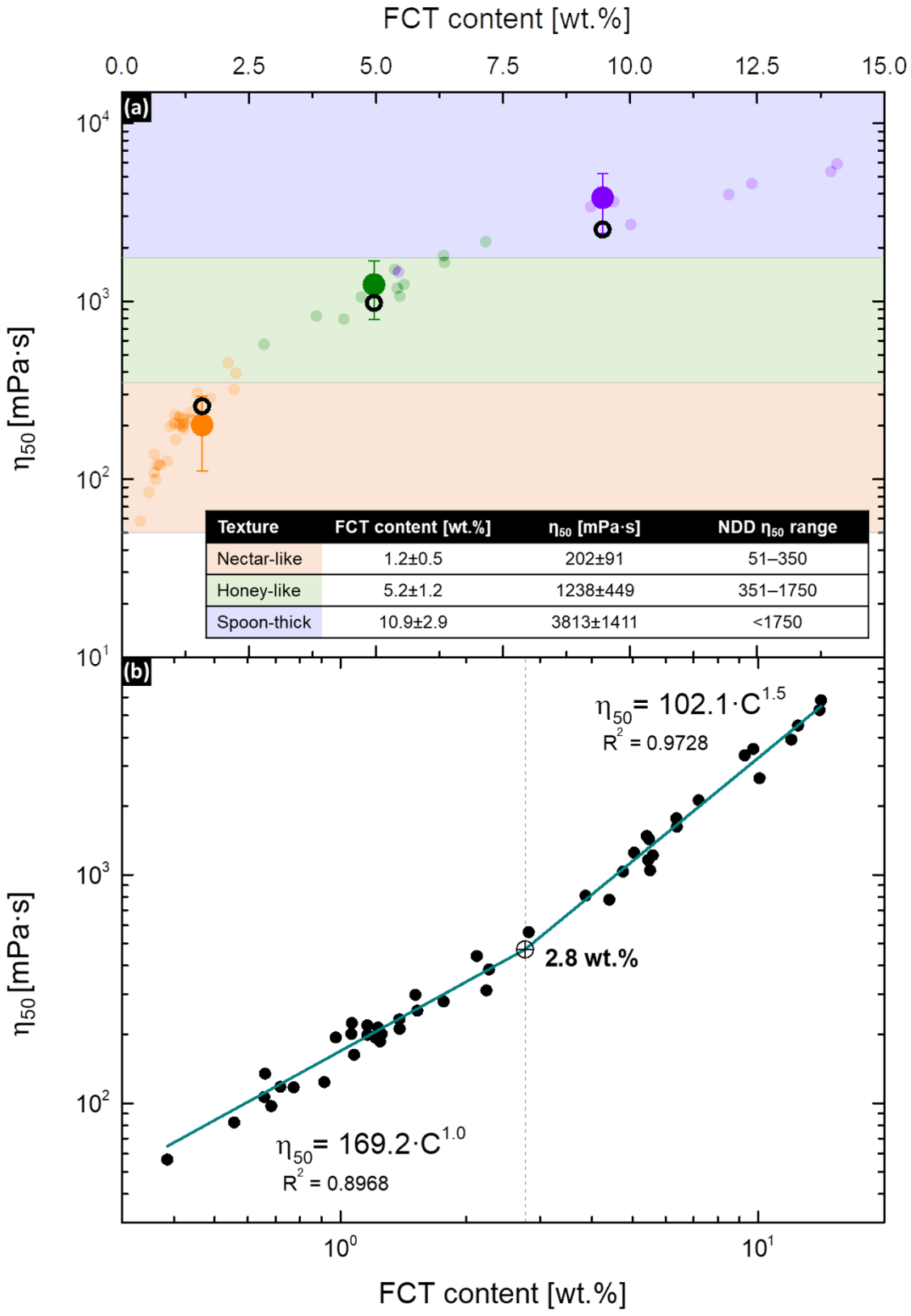

Figure 4. Viscosity at a shear rate of 50 s^{-1} and a temperature of 25 °C versus FCT content in water in (a) semi-log scale (bigger points represent mean values for each texture, and black unfilled points represent the average values of hand-prepared samples) and (b) log-log scale, fitted to intersecting power-law models

As can be seen from the figure, most of the values are within the recommended viscosity range, and only a few printed replicates, such as the intended honey-like sample showing the lowest viscosity of the spoon-thick texture (highest green point), or the intended spoon-thick sample showing the highest viscosity of the honey-like texture (lowest violet point), have textures different from the target ones. Above all, it must be emphasised that the averages of the viscosity values and their standard deviations are within the limits established for the three textures.

The η_{50} as a function of the concentration in a log-log scale (Figure b) follow a linear trend, corresponding to a power-law expression, with a change in slope at a concentration of approximately 2.8 wt.%. This type of viscosity dependence on concentration is very common in hydrocolloid solutions, with changes in slope (or intersection between different potential models) being taken as critical concentrations and boundaries between different concentration regimes. The overlap concentration (C*), which separates the diluted and semi-diluted unentangled regimes, and the entanglement concentration (C_e), which is the boundary between the semi-diluted unentangled/entangled regimes, are the critical concentrations most commonly found in polymer solutions, although more or less regions may be observed depending on the type of polymer (Pollard & Fischer, 2014; Wyatt & Liberatore, 2009; Zhang et al., 2016). Critical concentrations are usually obtained from the evaluation of zero-shear or specific viscosities and, because the increase in viscosity with concentration in shear-thinning fluids becomes less significant with increasing shear rate (Lapasin et al., 1995), the slopes obtained are smaller than those obtained in zero-shear conditions. Hence, the results obtained in this study are difficult to compare with those of previous studies, regarding the determination of the critical concentration. However, the critical concentration value found in this study (2.8 wt.%) is in good agreement with the entanglement concentrations of different starches (Li et al., 2016), which is, along with xanthan gum, one of the major components of FCT. On the contrary, the overlap concentration is usually found at much lower concentrations for starch and xanthan gum solutions (Wang et al., 2001; Wyatt & Liberatore, 2009).

As mentioned in the Introduction section, although the NDD criterion for classifying textures is only the viscosity at 50 s^{-1}, there are different shear rates to which foods and beverages are subjected to during swallowing (Brito-de la Fuente et al., 2012, 2019; Nutritional Aspects of Dysphagia Management, 2017; Qazi et al., 2019; Salinas-Vázquez et al., 2014). Therefore, it is interesting to evaluate the viscous flow properties of these products over a wide range of shear rates. Figure shows the shear rate dependence of the viscosity for some selected blends.

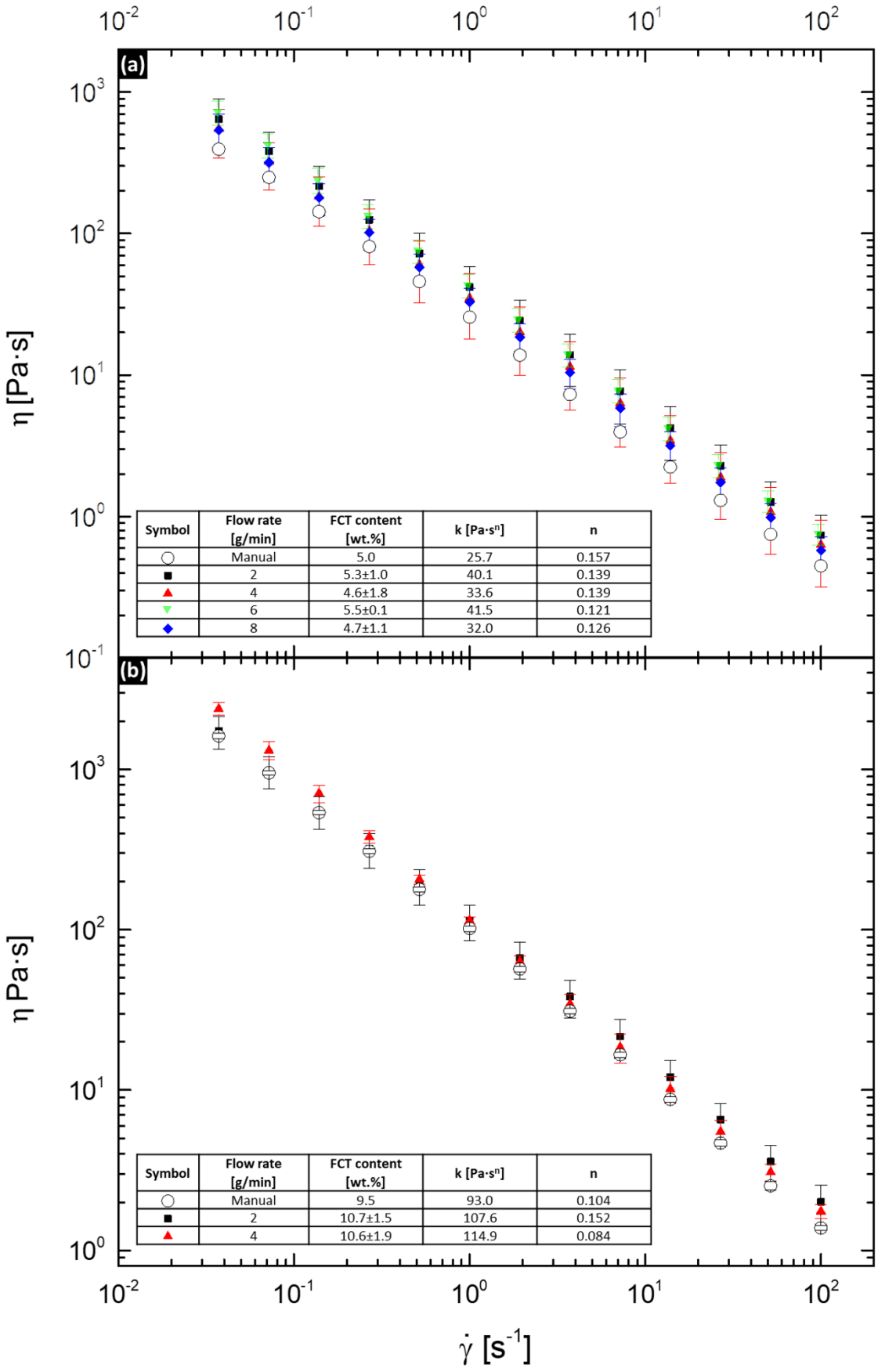

Figure 5. Flow curves and values of power-law fitting parameters for (a) nectar-like and (b) spoon-thick blends processed with the MIX3D accessory (solid symbols) and for hand-prepared blends (open symbols)

Independently from the printing flow rate, the MIX3D accessory generally provides thickened samples with viscosity values and shear rate dependence comparable to those prepared by hand. The flow curves included in Figure 4 correspond to the average data for each flow rate. The standard deviation of the viscosities is represented as error bars, whereas the variability of the thickener concentration is indicated in the legends. The legends of Figure 4 also shows the parameters resulting from the fitting of the different average flow curves to the power-law model performed as follows (the inclusion of the fittings has been avoided for the sake of clarity):

$$\eta = k\dot{\gamma}^{n-1} \,, \qquad [3]$$

where η is the apparent viscosity, $\dot{\gamma}$ is the shear rate, k is the consistency index, and n is the flow index. The power-law fitting parameters also reflect the previously discussed differences in η_{50}. The consistency index (k) is very sensitive to changes in concentration and, considering the fact that it represents the viscosity value at 1 s^{-1}, it also reflects the variations at low or moderate shear rates. Although the flow response of printed systems is very similar to that of hand-prepared ones, it is apparent that the former generally show slightly higher viscosity values than manually mixed blends, which could be due to the significantly lower bulk viscosity induced by the lower amount of air trapped in the printed samples, as illustrated in Figure .

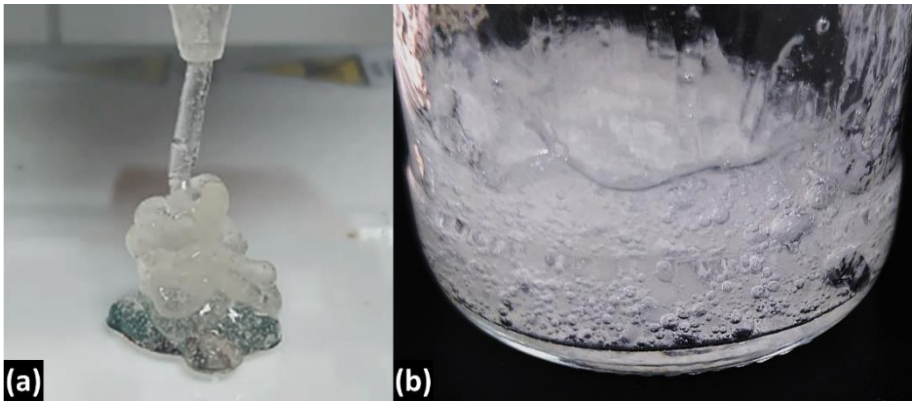

Figure 6. Images of spoon-thick blends (a) processed with MIX3D accessory and (b) prepared by hand

As a result, hand-mixed samples had lower viscosity than the MIX3D accessory processed samples with the same (or even lower) effective concentrations.

3.3. Linear viscoelasticity

The viscoelastic responses of the obtained blends in SAOS experiments were also analysed, and the results for selected blends printed at a 2 g/min flow rate are shown in Figure . The samples were subjected to frequency sweeps within the linear viscoelasticity regime. From Figure 6, it can be observed that the dependence of the moduli on frequency is weaker as the thickener concentration

increases, yielding gel-like responses, which evolve from soft gel, for the nectar-like texture, to a strong gel, for the spoon-thick consistency.

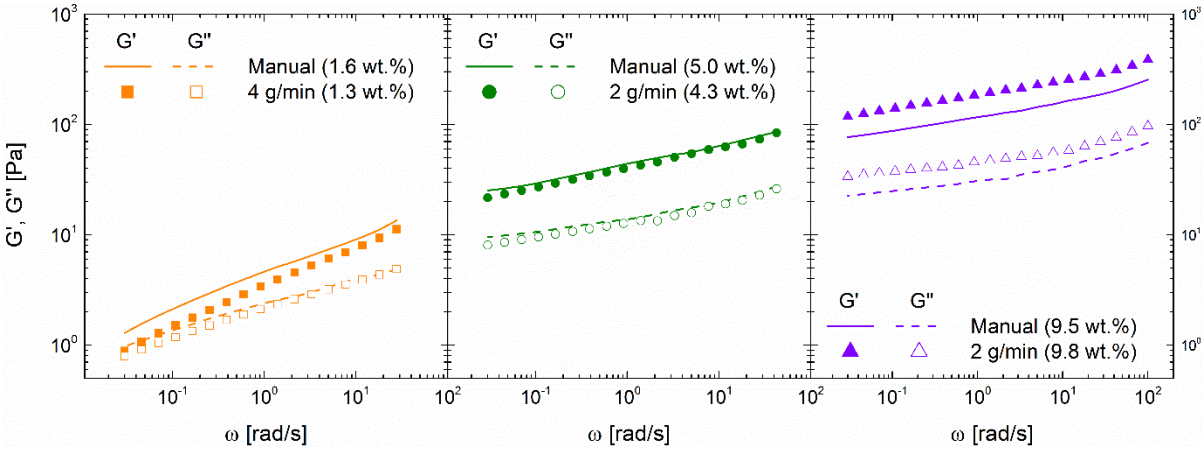

Figure 7. Viscoelastic response of FCT/water (a) nectar-like, (b) honey-like, and (c) spoon-thick blends processed with the MIX3D accessory

A well-developed plateau region, with low values of the slope of the plots of G' and G" as a function of the angular frequency, characteristic of strong gels, is apparent in the spoon-thick system, whereas a tendency to reach a crossover between the G' and G' curves can be observed at low frequencies for the nectar-like system. However, in all cases, a predominant solid-like behaviour is observed; in particular, the storage modulus (G') is higher than the loss modulus (G") over the entire frequency range considered. This confirms that the concentration of all the mixtures studied are above the overlap concentration because, below this concentration, the diluted solutions must show a viscoelastic response characterised by G" values higher than G' in a wide frequency range as well as a high dependence of both SAOS functions on the frequency (Sworn, 2007).

Again, samples obtained with the MIX3D accessory show values of both moduli very close to those of the samples obtained by manual mixing, despite having a FCT content sometimes lower than that of hand-mixed samples. However, blends with spoon-thick textures processing with the MIX3D accessory generally have higher SAOS moduli than those obtained by manual mixing, probably owing to the lower amount of air bubbles incorporated, as discussed in the previous section.

3.4. Thickening of common beverages

The MIX3D accessory was also used to thicken both commercial orange juice and skimmed milk (see Movie M2 in the Supporting Information). Samples were mixed at 2 g/min to obtain the spoon-thick target texture, as this is the most interesting consistency to take advantage of all features of 3D printing. Figure shows plots of the viscosity and linear viscoelasticity as functions of the shear rate/frequency of the FCT-thickened orange juice, skimmed milk, and water obtained with the MIX3D accessory and by manual mixing.

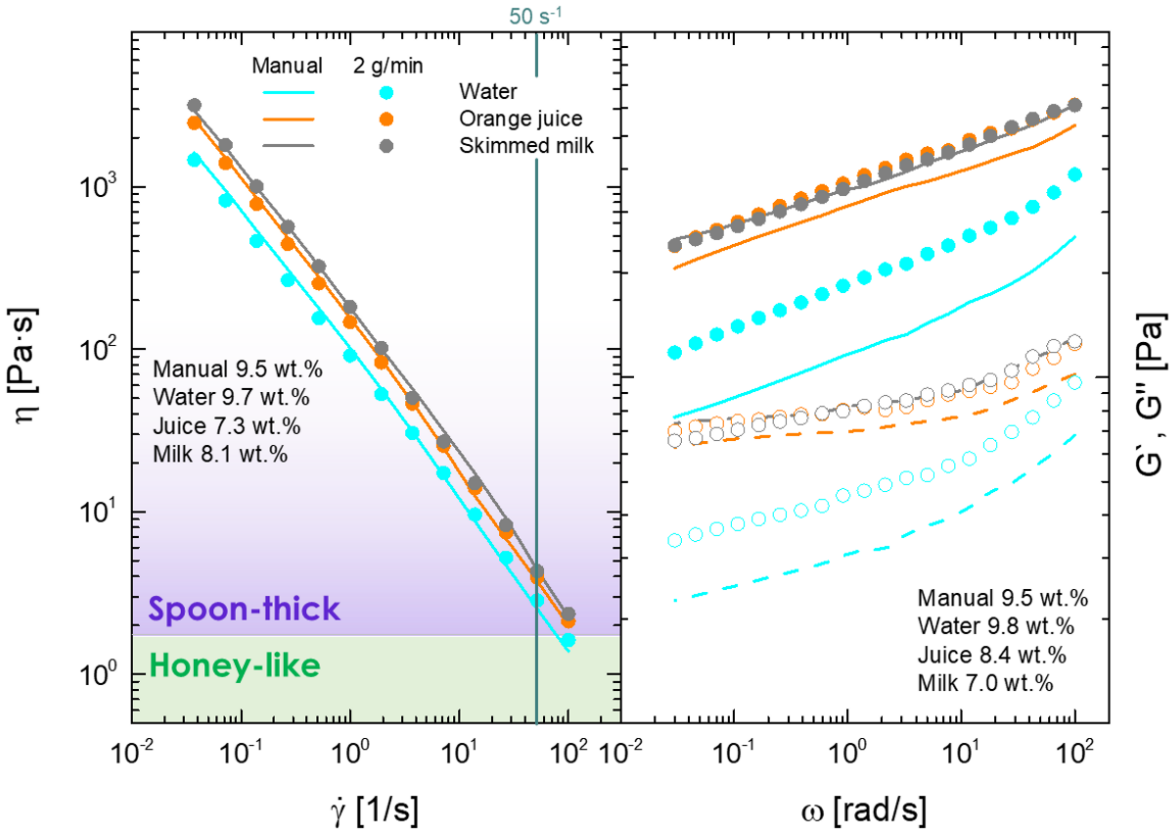

Figure 8. (a) Viscosity vs. shear rate and (b) linear viscoelastic functions vs. frequency of FCT-thickened orange juice, skimmed milk, and water

From Figure 8, it can be seen that higher values of viscosity and linear viscoelastic functions are obtained for thickened juice and milk than for thickened water. This is not surprising because the influence of the dispersing fluid on the rheological properties of thickened fluids is a well-known issue; the thickening effect of a given hydrocolloid is different for different dispersing media (Moret-Tatay et al., 2015; Sopade et al., 2007; Sopade, Halley, Cichero, Ward, Hui, et al., 2008; Sopade, Halley, Cichero, Ward, Liu, et al., 2008).

The most remarkable aspect of these results is that, by using the MIX3D accessory, similar viscous and linear viscoelastic responses to those obtained by manual mixing may be obtained, although a lower amount of thickener is needed (see inlets in Figure 8). More specifically, similar viscosity and linear viscoelastic values as those shown by a 9.5 wt.% hand-prepared thickened milk have been achieved by using 8.1 wt.% (for viscosity) and a 7.0 wt.% (for linear viscoelasticity functions) skimmed milk, respectively, with the mixing accessory. In the case of orange juice, the viscosity of the manually thickened fluid was matched by using a 7.3 wt.% thickener concentration. On the other hand, the 8.4 wt.% thickener mixed with the accessory has storage and loss moduli values slightly higher than those of the manually mixed 9.5 wt.% thickener.

A good example of how thickened fluids can be used to produce foods with an attractive appearance or simulated conventional foods is the “fried egg” for which the printing process is shown in Figure 2 and Movie M1 (Supporting Information). This model has been produced with skimmed milk (egg white) and orange juice (egg yolk) thickened to spoon-thick consistency, at a flow rate of approximately 2 g/min (10 mm/s print speed at 1/26/73 mixing ratios), a layer height of 1 mm and a line width of 2 mm, according to the size of the outlet orifice of the device.

Of course, it would be more appropriate to use base fluids that provide a taste more similar to that of a real fried egg, but this example adequately illustrates how this technology can be very useful for the preparation of appealing dysphagia-oriented products.

4. Concluding remarks

The in situ mixing of solid and liquid feeds during a continuous 3D printing process was successfully achieved in this study. The accessory was shown to successfully thicken water, orange juice, and skimmed milk. However, there are still some fluctuations in the final thickener concentration as well as in the flow of the mixture along the device, which are mainly due to the stickiness and high viscosity of the product during mixing and therefore become more evident as the solid content increases. However, these fluctuations are low enough to achieve viscosity values within the range required for each texture (nectar-like, honey-like, and spoon-thick). This aspect should be further improved for future adaptations to new viscosity classifications requiring higher viscosities or more precise control of the final consistency. Furthermore, the introduction of air into the blends prepared with the accessory is minimal compared to that observed in the manual preparation, resulting in slightly higher viscosities and more homogeneous and transparent blends.

Overall, the results of this study validate the proposed MIX3D accessory for the development of dysphagia-oriented products for in-situ application. The proposed accessory overcomes the limitations of the *in situ* mixing of solids and liquids. The proposed accessory is compatible with and operated by the firmware and hardware of a 3D printer and allows the implementation of additional feeds without complications, as well as the automatic and simple processing of foods with controlled rheological characteristics. This makes it possible the design of foods with appetising colours, odours, tastes and attractive shapes to favour patient acceptance.

5. References

American Dietetic Association. (2002). *National Dysphagia Diet: Standardization for Optimal Care*. American Dietetic Association. https://books.google.es/books?id=MZ5mSbGPOE4C

Andersen, U. T., Beck, A. M., Kjaersgaard, A., Hansen, T., & Poulsen, I. (2013). Systematic review and

evidence based recommendations on texture modified foods and thickened fluids for adults (≥18 years) with oropharyngeal dysphagia. *E-SPEN Journal*, *8*(4), e127–e134. https://doi.org/10.1016/j.clnme.2013.05.003

Attrill, S., White, S., Murray, J., Hammond, S., & Doeltgen, S. (2018). Impact of oropharyngeal dysphagia on healthcare cost and length of stay in hospital: A systematic review. In *BMC Health Services Research* (Vol. 18, Issue 1, p. 594). BioMed Central Ltd. https://doi.org/10.1186/s12913-018-3376-3

Baijens, L. W. J., Walshe, M., Aaltonen, L. M., Arens, C., Cordier, R., Cras, P., Crevier-Buchman, L., Curtis, C., Golusinski, W., Govender, R., Eriksen, J. G., Hansen, K., Heathcote, K., Hess, M. M., Hosal, S., Klussmann, J. P., Leemans, C. R., MacCarthy, D., Manduchi, B., … Clavé, P. (2021). European white paper: oropharyngeal dysphagia in head and neck cancer. *European Archives of Oto-Rhino-Laryngology*, *278*(2), 577–616. https://doi.org/10.1007/s00405-020-06507-5

Bolivar-Prados, M., Rofes, L., Arreola, V., Guida, S., Nascimento, W. V., Martin, A., Vilardell, N., Ortega Fernández, O., Ripken, D., Lansink, M., & Clavé, P. (2019). Effect of a gum-based thickener on the safety of swallowing in patients with poststroke oropharyngeal dysphagia. *Neurogastroenterology & Motility*, *31*(11). https://doi.org/10.1111/nmo.13695

Brito-de la Fuente, E., Staudinger-Prevost, N., Quinchia, L. A., Valencia, C., Partal, P., Franco, J. M., & Gallegos, C. (2012). Design of a New Spoon-Thick Consistency Oral Nutrition Supplement Using Rheological Similarity with a Swallow Barium Test Feed. *Applied Rheology*, *22*(5), 53365. https://doi.org/https://doi.org/10.3933/applrheol-22-53365

Brito-de la Fuente, E., Turcanu, M., Ekberg, O., & Gallegos, C. (2019). *Rheological Aspects of Swallowing and Dysphagia: Shear and Elongational Flows BT - Dysphagia: Diagnosis and Treatment* (O. Ekberg (ed.); pp. 687–716). Springer International Publishing. https://doi.org/10.1007/174_2017_119

Cabré, M., Serra-Prat, M., Force, L., Almirall, J., Palomera, E., & Clavé, P. (2013). Oropharyngeal Dysphagia is a Risk Factor for Readmission for Pneumonia in the Very Elderly Persons: Observational Prospective Study. *The Journals of Gerontology: Series A*, *69A*(3), 330–337. https://doi.org/10.1093/gerona/glt099

Carrión, S., Costa, A., Ortega, O., Verin, E., Clavé, P., & Laviano, A. (2019). *Complications of Oropharyngeal Dysphagia: Malnutrition and Aspiration Pneumonia BT - Dysphagia: Diagnosis and Treatment* (O. Ekberg (ed.); pp. 823–857). Springer International Publishing. https://doi.org/10.1007/174_2017_168

Choi, K. H., Ryu, J. S., Kim, M. Y., Kang, J. Y., & Yoo, S. D. (2011). Kinematic analysis of dysphagia: Significant parameters of aspiration related to bolus viscosity. *Dysphagia*, *26*(4), 392–398.

https://doi.org/10.1007/s00455-011-9325-5

Cichero, J. A. Y., Steele, C., Duivestein, J., Clavé, P., Chen, J., Kayashita, J., Dantas, R., Lecko, C., Speyer, R., Lam, P., & Murray, J. (2013). The Need for International Terminology and Definitions for Texture-Modified Foods and Thickened Liquids Used in Dysphagia Management: Foundations of a Global Initiative. *Current Physical Medicine and Rehabilitation Reports*, *1*(4), 280–291. https://doi.org/10.1007/s40141-013-0024-z

Clavé, P., De Kraa, M., Arreola, V., Girvent, M., Farré, R., Palomera, E., & Serra-Prat, M. (2006). The effect of bolus viscosity on swallowing function in neurogenic dysphagia. *Alimentary Pharmacology and Therapeutics*, *24*(9), 1385–1394. https://doi.org/10.1111/j.1365-2036.2006.03118.x

Clavé, Pere, & Shaker, R. (2015). Dysphagia: Current reality and scope of the problem. In *Nature Reviews Gastroenterology and Hepatology* (Vol. 12, Issue 5, pp. 259–270). Nature Publishing Group. https://doi.org/10.1038/nrgastro.2015.49

Colodny, N. (2005). Dysphagic Independent Feeders' Justifications for Noncompliance With Recommendations by a Speech-Language Pathologist. *American Journal of Speech-Language Pathology*. https://doi.org/10.1044/1058-0360(2005/008)

Diañez, I., Gallegos, C., Brito-de la Fuente, E., Martínez, I., Valencia, C., Sánchez, M. C., Diaz, M. J., & Franco, J. M. (2019). 3D printing in situ gelification of κ-carrageenan solutions: Effect of printing variables on the rheological response. *Food Hydrocolloids*, *87*, 321–330. https://doi.org/10.1016/j.foodhyd.2018.08.010

Fresubin Clear Thickener – Caring for Life. (n.d.). Retrieved January 25, 2021, from https://www.caringforlife.hk/index.php/en/products/by-indication/fresubin-clear-thickener/

Nutritional Aspects of Dysphagia Management, 81 Advances in Food and Nutrition Research 271 (2017). https://www.sciencedirect.com/science/article/pii/S1043452616300687

Herranz, B., Criado, C., Pozo-Bayón, M. Á., & Álvarez, M. D. (2021). Effect of addition of human saliva on steady and viscoelastic rheological properties of some commercial dysphagia-oriented products. *Food Hydrocolloids*, *111*, 106403. https://doi.org/10.1016/j.foodhyd.2020.106403

Inamoto, Y., Saitoh, E., Okada, S., Kagaya, H., Shibata, S., Ota, K., Baba, M., Fujii, N., Katada, K., Wattanapan, P., & Palmer, J. B. (2013). The effect of bolus viscosity on laryngeal closure in swallowing: Kinematic analysis using 320-row area detector CT. *Dysphagia*, *28*(1), 33–42. https://doi.org/10.1007/s00455-012-9410-4

Lapasin, R., Pricl, S., Lapasin, R., & Pricl, S. (1995). Industrial applications of polysaccharides. In *Rheology of Industrial Polysaccharides: Theory and Applications* (pp. 134–161). Springer US. https://doi.org/10.1007/978-1-4615-2185-3_2

526 Leonard, R. J., White, C., McKenzie, S., & Belafsky, P. C. (2014). Effects of bolus rheology on
527 aspiration in patients with dysphagia. *Journal of the Academy of Nutrition and Dietetics*, *114*(4),
528 590–594. https://doi.org/10.1016/j.jand.2013.07.037
529 Li, X., Chen, H., & Yang, B. (2016). Centrifugally spun starch-based fibers from amylopectin rich
530 starches. *Carbohydrate Polymers*, *137*, 459–465. https://doi.org/10.1016/j.carbpol.2015.10.079
531 Lim, D. J. H., Mulkerrin, S. M., Mulkerrin, E. C., & O'Keeffe, S. T. (2016). A randomised trial of the
532 effect of different fluid consistencies used in the management of dysphagia on quality of life: a
533 time trade-off study. *Age and Ageing*, *45*(2), 309–312. https://doi.org/10.1093/ageing/afv194
534 Low, J., Wyles, C., Wilkinson, T., & Sainsbury, R. (2001). The effect of compliance on clinical
535 outcomes for patients with dysphagia on videofluoroscopy. *Dysphagia*, *16*(2), 123–127.
536 https://doi.org/10.1007/s004550011002
537 Moret-Tatay, A., Rodríguez-García, J., Martí-Bonmatí, E., Hernando, I., & Hernández, M. J. (2015).
538 Commercial thickeners used by patients with dysphagia: Rheological and structural behaviour
539 in different food matrices. *Food Hydrocolloids*, *51*, 318–326.
540 https://doi.org/10.1016/j.foodhyd.2015.05.019
541 Newman, R., Vilardell, N., Clavé, P., & Speyer, R. (2016). Effect of Bolus Viscosity on the Safety and
542 Efficacy of Swallowing and the Kinematics of the Swallow Response in Patients with
543 Oropharyngeal Dysphagia: White Paper by the European Society for Swallowing Disorders
544 (ESSD). In *Dysphagia* (Vol. 31, Issue 2, pp. 232–249). Springer New York LLC.
545 https://doi.org/10.1007/s00455-016-9696-8
546 Ortega, O., Bolívar-Prados, M., Arreola, V., Nascimento, W. V., Tomsen, N., Gallegos, C., Brito-de La
547 Fuente, E., & Clavé, P. (2020). Therapeutic Effect, Rheological Properties and α-Amylase
548 Resistance of a New Mixed Starch and Xanthan Gum Thickener on Four Different Phenotypes of
549 Patients with Oropharyngeal Dysphagia. *Nutrients*, *12*(6), 1873.
550 https://doi.org/10.3390/nu12061873
551 Pollard, M. A., & Fischer, P. (2014). Semi-dilute galactomannan solutions: observations on viscosity
552 scaling behavior of guar gum. *Journal of Physics: Condensed Matter*, *26*(46), 464107.
553 https://doi.org/10.1088/0953-8984/26/46/464107
554 Qazi, W. M., Ekberg, O., Wiklund, J., Kotze, R., & Stading, M. (2019). Assessment of the Food-
555 Swallowing Process Using Bolus Visualisation and Manometry Simultaneously in a Device that
556 Models Human Swallowing. In *Dysphagia* (Vol. 34, Issue 6, pp. 821–833). Springer New York
557 LLC. https://doi.org/10.1007/s00455-019-09995-8
558 Quinchia, L. A., Valencia, C., Partal, P., Franco, J. M., Brito-de la Fuente, E., & Gallegos, C. (2011).
559 Linear and non-linear viscoelasticity of puddings for nutritional management of dysphagia.

560 *Food Hydrocolloids*, *25*(4), 586–593. https://doi.org/10.1016/j.foodhyd.2010.07.006
561 Salinas-Vázquez, M., Vicente, W., Brito-de la Fuente, E., Gallegos, C., Márquez, J., & Ascanio, G.
562 (2014). Early Numerical Studies on the Peristaltic Flow through the Pharynx. *Journal of Texture*
563 *Studies*, *45*(2), 155–163. https://doi.org/10.1111/jtxs.12060
564 Shaker, R. (2006). Oropharyngeal Dysphagia. *Gastroenterology & Hepatology*, *2*(9), 633–634.
565 https://pubmed.ncbi.nlm.nih.gov/28316533
566 Sopade, P. A., Halley, P. J., Cichero, J. A. Y., & Ward, L. C. (2007). Rheological characterisation of food
567 thickeners marketed in Australia in various media for the management of dysphagia. I: Water
568 and cordial. *Journal of Food Engineering*, *79*(1), 69–82.
569 https://doi.org/10.1016/j.jfoodeng.2006.01.045
570 Sopade, P. A., Halley, P. J., Cichero, J. A. Y., Ward, L. C., Hui, L. S., & Teo, K. H. (2008). Rheological
571 characterisation of food thickeners marketed in Australia in various media for the management
572 of dysphagia. II. Milk as a dispersing medium. *Journal of Food Engineering*, *84*(4), 553–562.
573 https://doi.org/10.1016/j.jfoodeng.2007.06.024
574 Sopade, P. A., Halley, P. J., Cichero, J. A. Y., Ward, L. C., Liu, J., & Varliveli, S. (2008). Rheological
575 characterization of food thickeners marketed in Australia in various media for the management
576 of dysphagia. III. Fruit juice as a dispersing medium. *Journal of Food Engineering*, *86*(4), 604–
577 615. https://doi.org/10.1016/j.jfoodeng.2007.11.013
578 Sworn, G. (2007). Natural Thickeners. In *Handbook of Industrial Water Soluble Polymers* (pp. 10–31).
579 Blackwell Publishing Ltd. https://doi.org/10.1002/9780470988701.ch2
580 Turcanu, M., Siegert, N., Secouard, S., Brito-de la Fuente, E., Balan, C., & Gallegos, C. (2018). An
581 alternative elongational method to study the effect of saliva on thickened fluids for dysphagia
582 nutritional support. *Journal of Food Engineering*, *228*, 79–83.
583 https://www.sciencedirect.com/science/article/pii/S0260877418300700
584 Wang, F., Sun, Z., & Wang, Y. J. (2001). Study of xanthan gum/waxy corn starch interaction in
585 solution by viscometry. *Food Hydrocolloids*, *15*(4–6), 575–581. https://doi.org/10.1016/S0268-
586 005X(01)00065-0
587 Wyatt, N. B., & Liberatore, M. W. (2009). Rheology and viscosity scaling of the polyelectrolyte
588 xanthan gum. *Journal of Applied Polymer Science*, *114*(6), 4076–4084.
589 https://doi.org/10.1002/app.31093
590 Zhang, E., Dai, X., Dong, Z., Qiu, X., & Ji, X. (2016). Critical concentration and scaling exponents of one
591 soluble polyimide - From dilute to semidilute entangled solutions. *Polymer*, *84*, 275–285.
592 https://doi.org/10.1016/j.polymer.2016.01.001
593

Figure

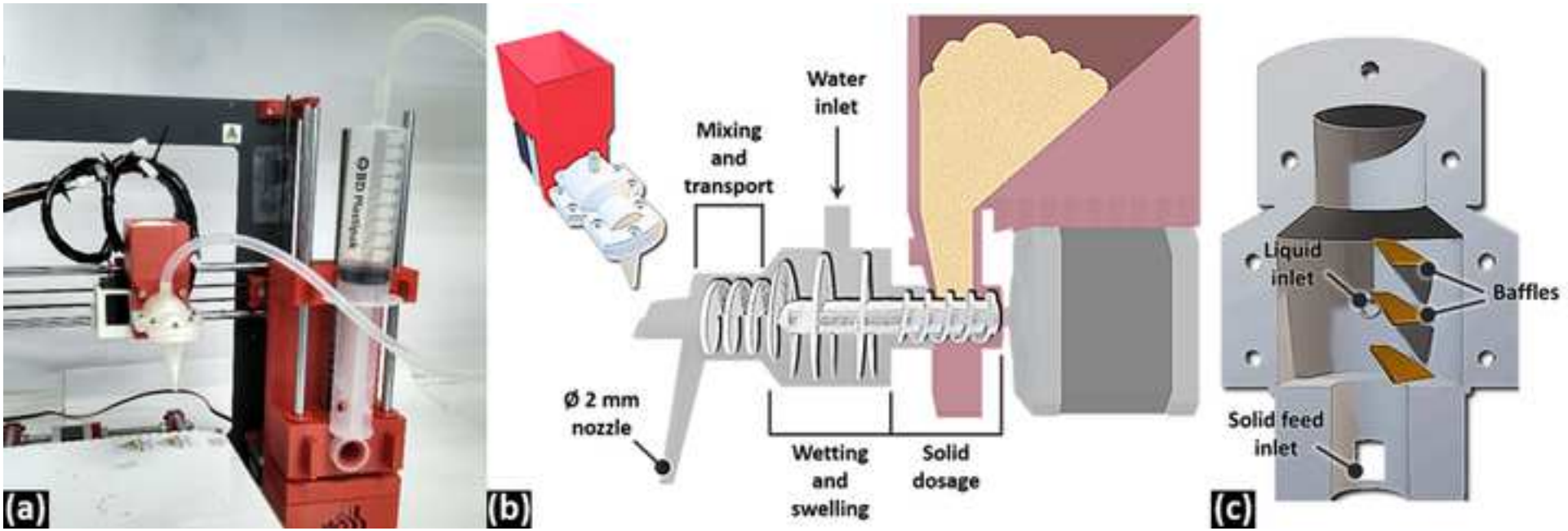

Figure

Click here to access/download;Figure;FIG2.tif

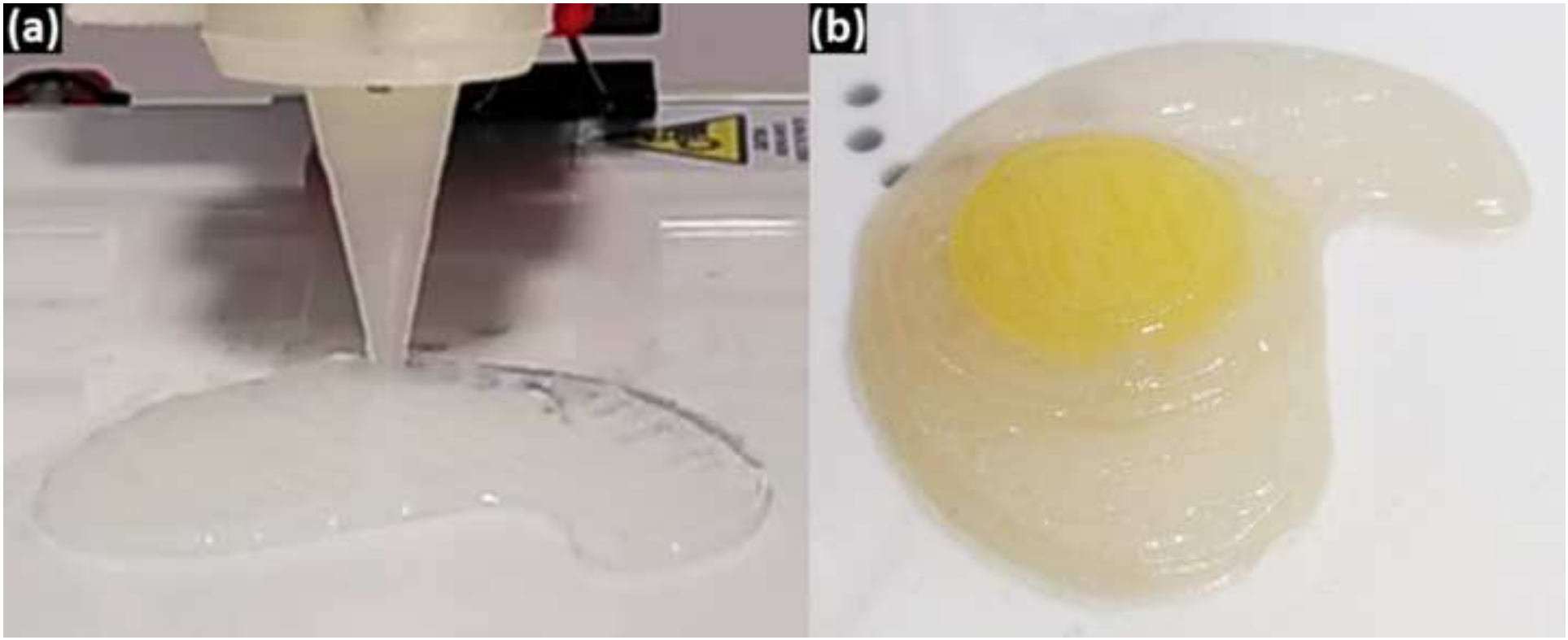

Figure

Click here to access/download;Figure;FIG3.tif

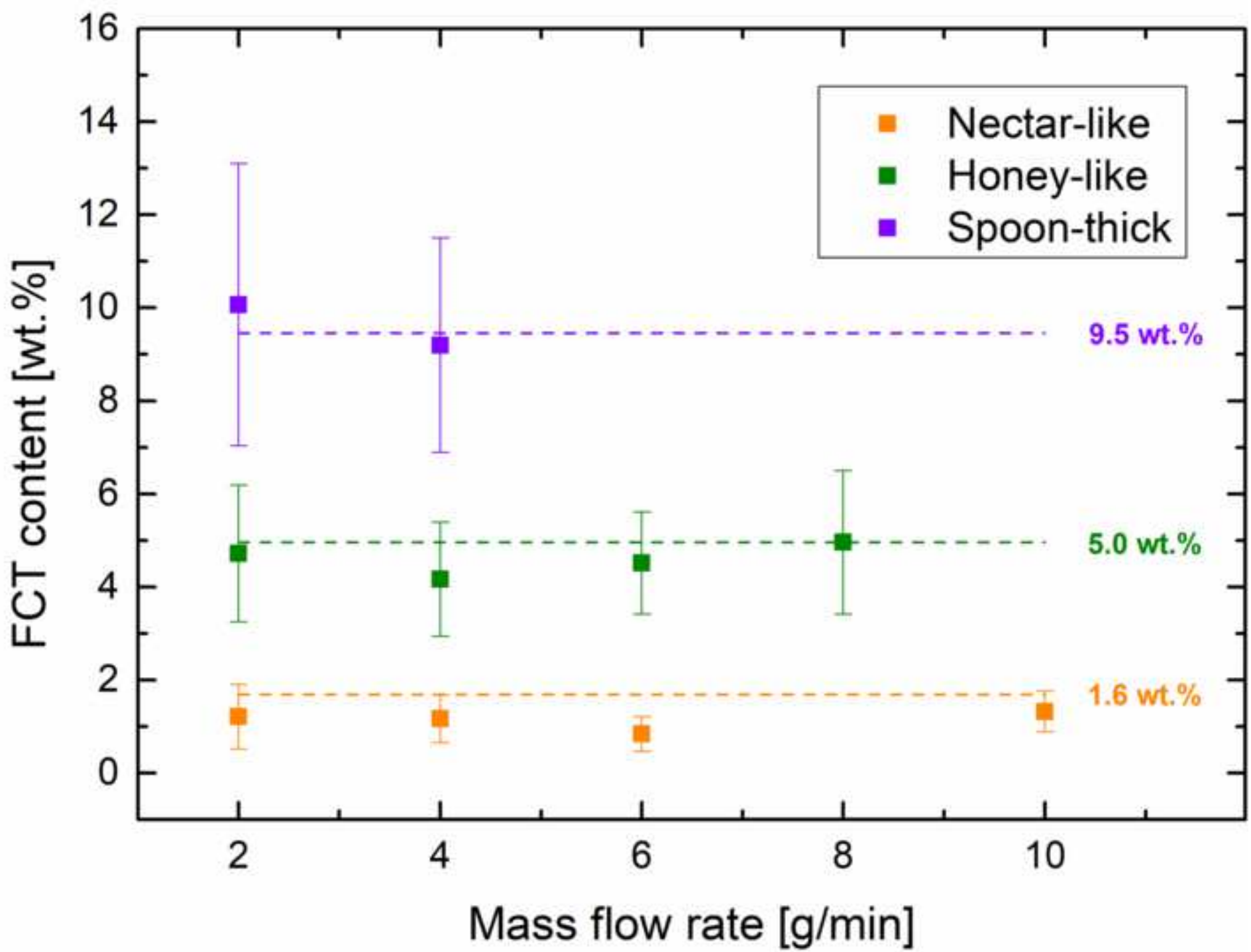

Figure

Click here to access/download;Figure;FIG4v2.tif

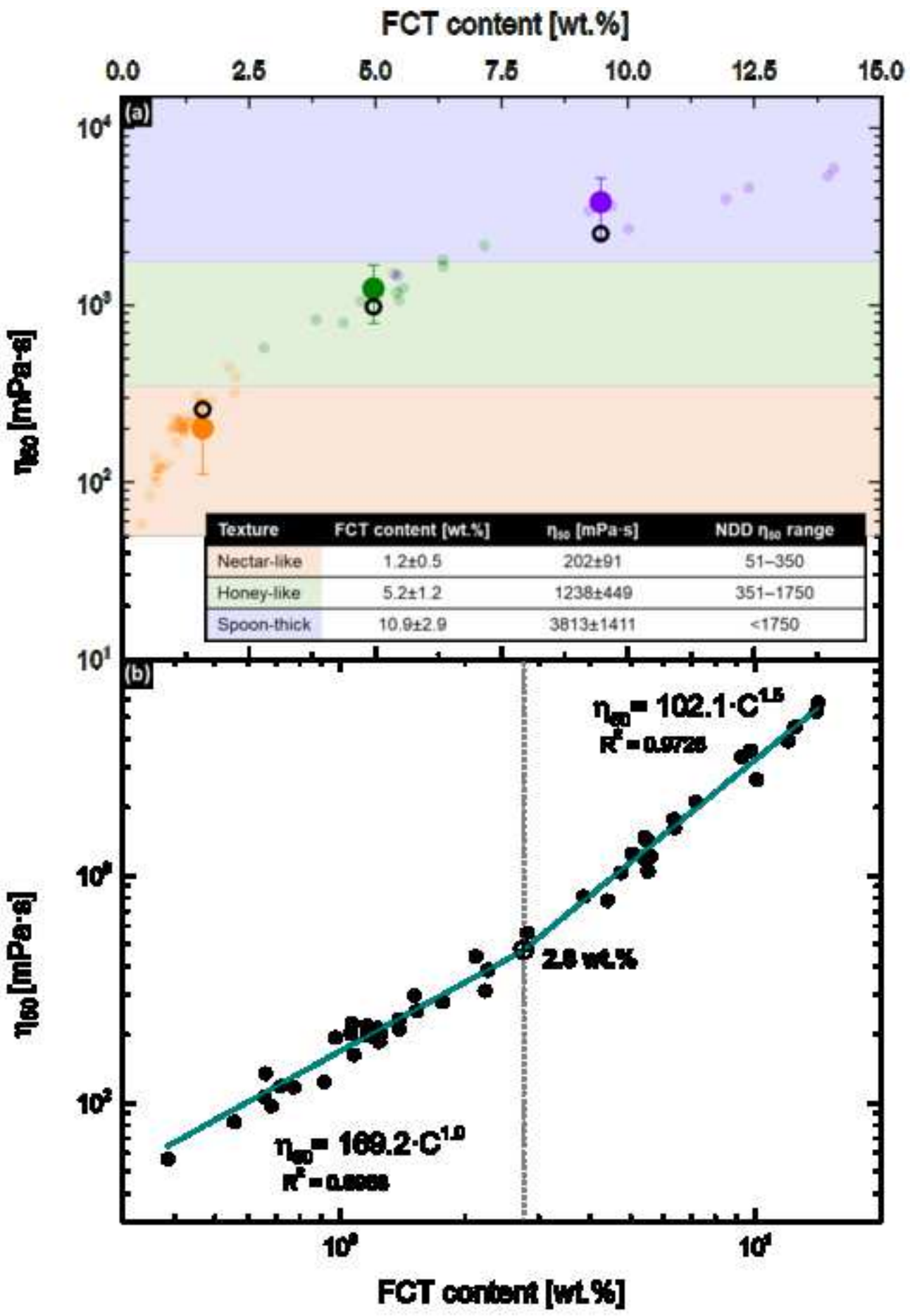

Figure

Click here to access/download;Figure;FIG5v2.tif

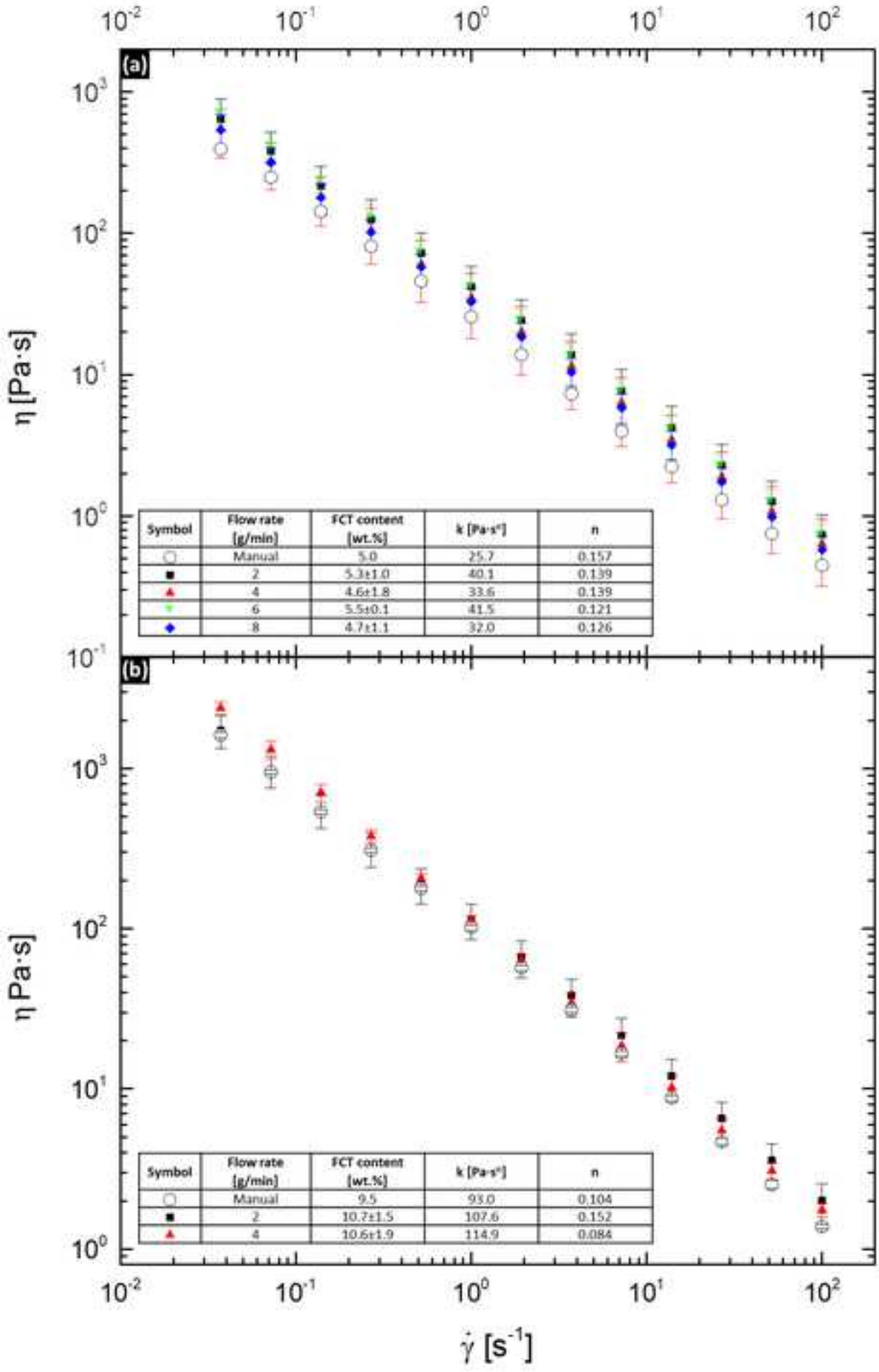

Figure

Click here to access/download;Figure;FIG6.tif

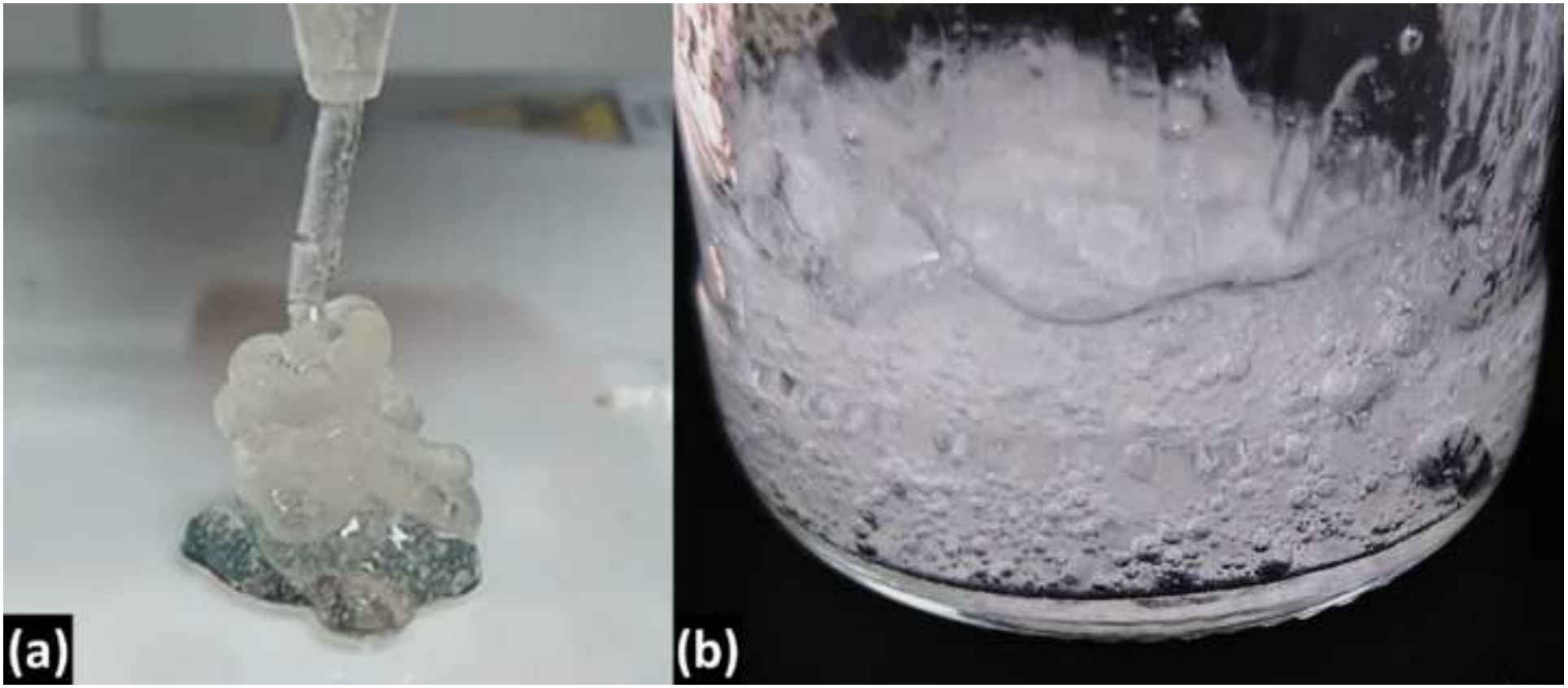

Figure

Click here to access/download;Figure;FIG7v2.tif

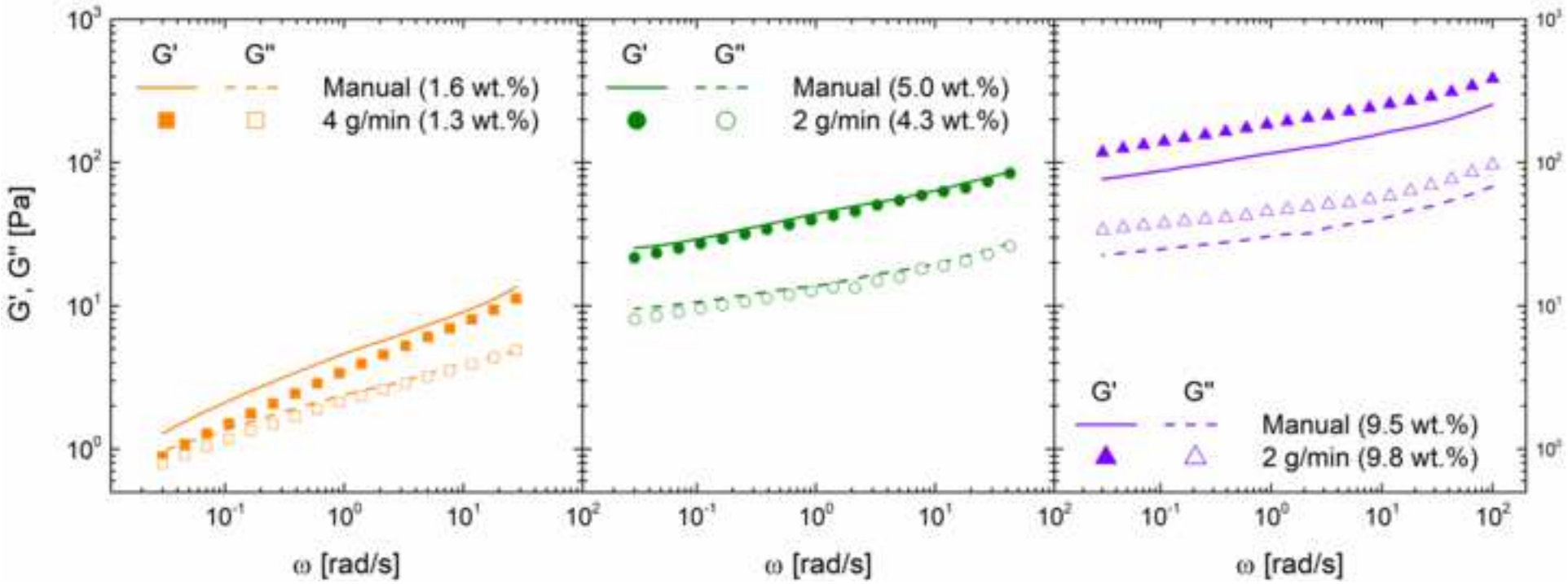

Figure

Click here to access/download;Figure;FIG8.tif